Supporting Information

Quasi-solid Electrolyte Based on Cost-effective Sodium Salt for High-performance Sodium-ion Supercapacitors

Natthawut Suebsing[a], Kornkanok Noulta[b], Channarong Puchongkawarin[c], Oruethai Jaiboon[a], Adulvit Chuaephon[d], Arisa Phukhrongthung[e], and Santamon Luanwuthi[e,*]

[a] *Department of Physics, Faculty of Science, Ubon Ratchathani University, Ubon Ratchathani 34190, Thailand.*

[b] *Department of Chemistry, Faculty of Science, Ubon Ratchathani University, Ubon Ratchathani 34190, Thailand.*

[c] *Department of Chemical Engineering, Faculty of Engineering, Ubon Ratchathani University, Ubon Ratchathani 34190, Thailand.*

[d] *Department of Physics, Faculty of Science, Khon Kaen University, Khon Kaen 40002, Thailand.*

[e] *Department of Industrial Engineering, Faculty of Engineering, Ubon Ratchathani University, Ubon Ratchathani 34190, Thailand.*

*Corresponding author.

Email address: santamon.l@ubu.ac.th

Deconvolution of FTIR spectra

To study the transport property of the as-prepared QSEs, the FTIR deconvolution technique was carried out by converting the FTIR spectra of each QSE into absorbance mode. Subsequently, the deconvolution peaks were fitted by using Voigt area function. The area under the deconvoluted peaks was used to calculate free ions using the following equation [1]:

$$Free\ ions\ \ (\%) = \frac{A_f}{A_f + A_c} \times 100\% \tag{S1}$$

where A_f and A_c represent the area of free and contact ions, respectively.

The parameters of ion transport influencing the ionic conductivity of QSEs, including the number density (η), ionic mobility (μ) and diffusion coefficient (D) were determined using the following expression [2-4]:

$$\eta = \frac{M \times N_A}{V_T} \times Free\ ions \tag{S2}$$

$$\mu = \frac{\sigma}{\eta e} \tag{S3}$$

$$D = \frac{\mu k_B T}{e} \tag{S4}$$

where M is the moles of each PEG wt%, N_A represents the Avogadro's number (6.02×10^{23} mol^{-1}), V_T (cm^3) is the volume, T (K) is the absolute temperature, σ (S/cm) is the ionic conductivity, e is the electric charge (1.6×10^{-19} C), and k_B denotes the Boltzmann constant (1.38×10^{-23} J/K).

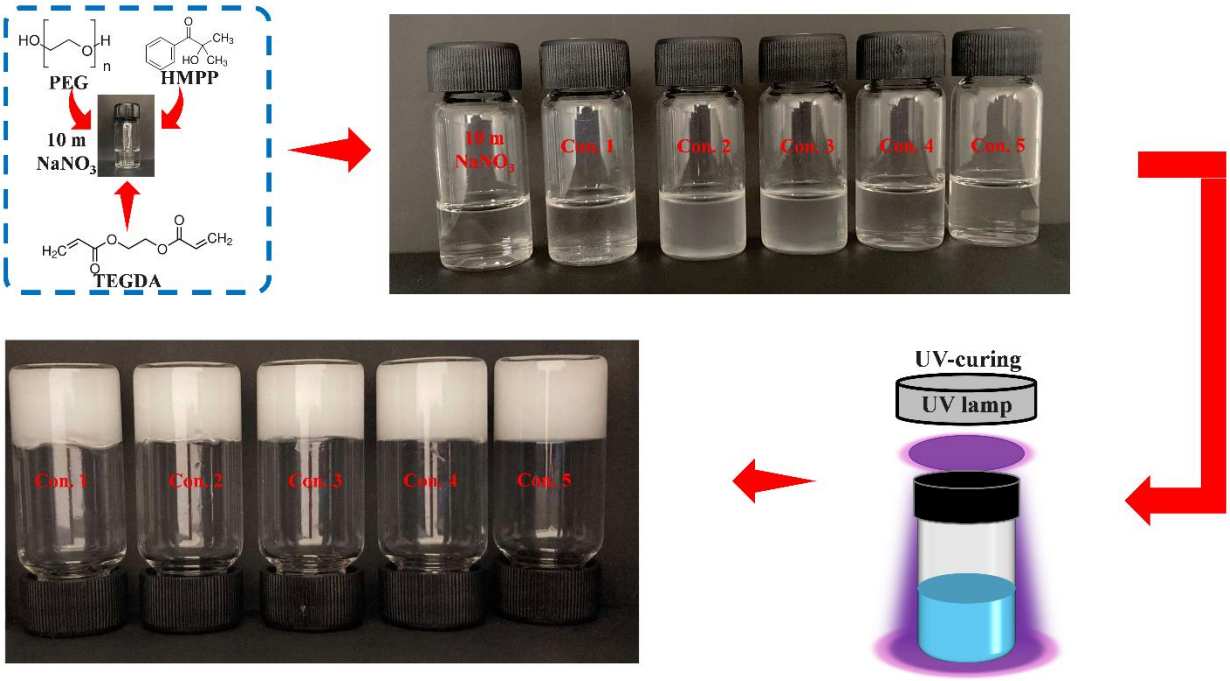

Figure S1. Schematic of QSEs preparation via UV irradiation process.

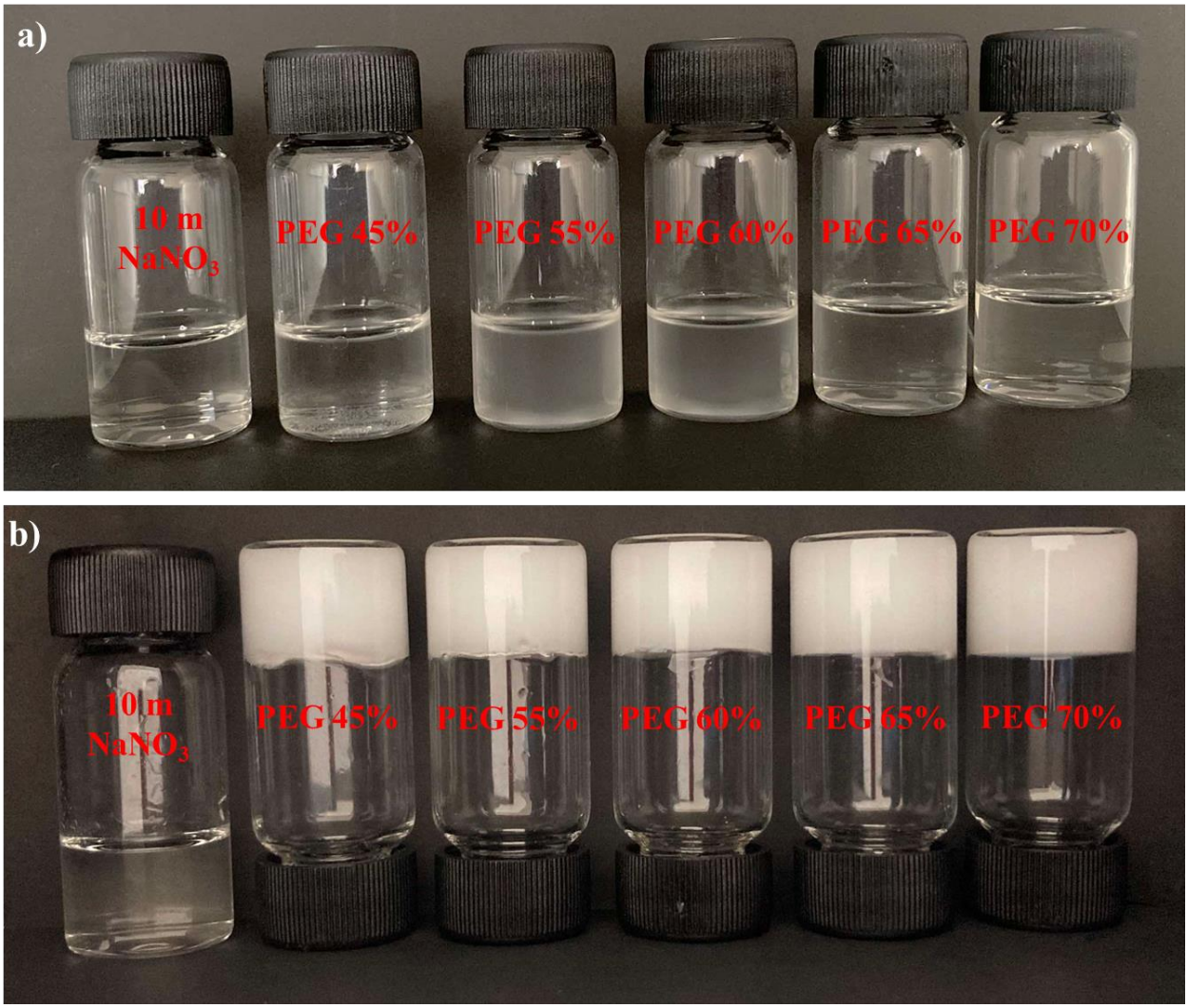

Figure S2. a) Photograph of precursor solutions with different PEG contents and b) Comparison of 10 m $NaNO_3$ and the as-prepared QSEs.

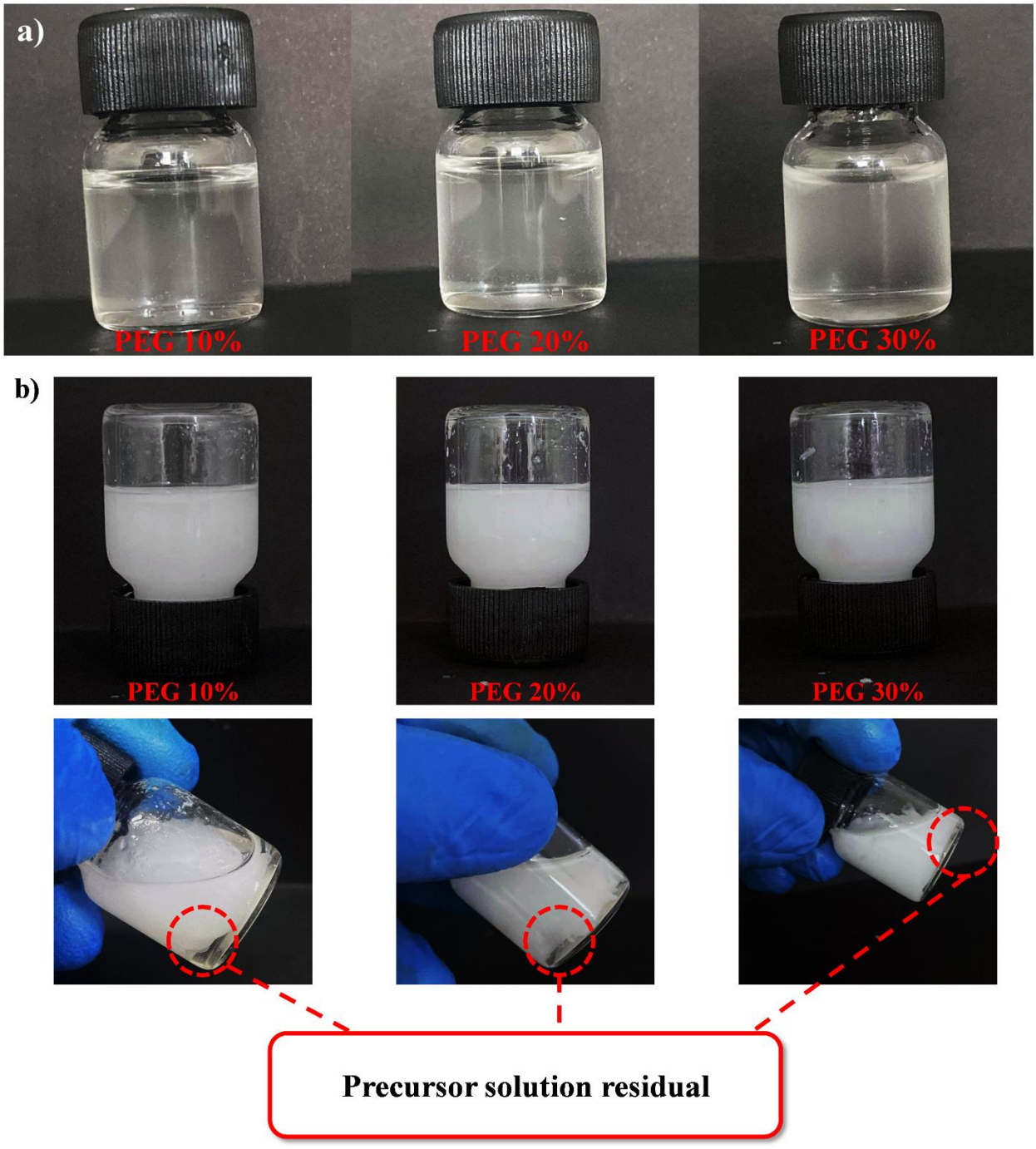

Figure S3. a) Photograph of precursor solutions with different PEG contents below 45 wt% and b) incomplete preparation of QSEs after UV-curing with the different PEG contents of 10, 20, and 30 wt%, resulting from insufficient mixing between the components at PEG contents below 45 wt% and 10 m $NaNO_3$.

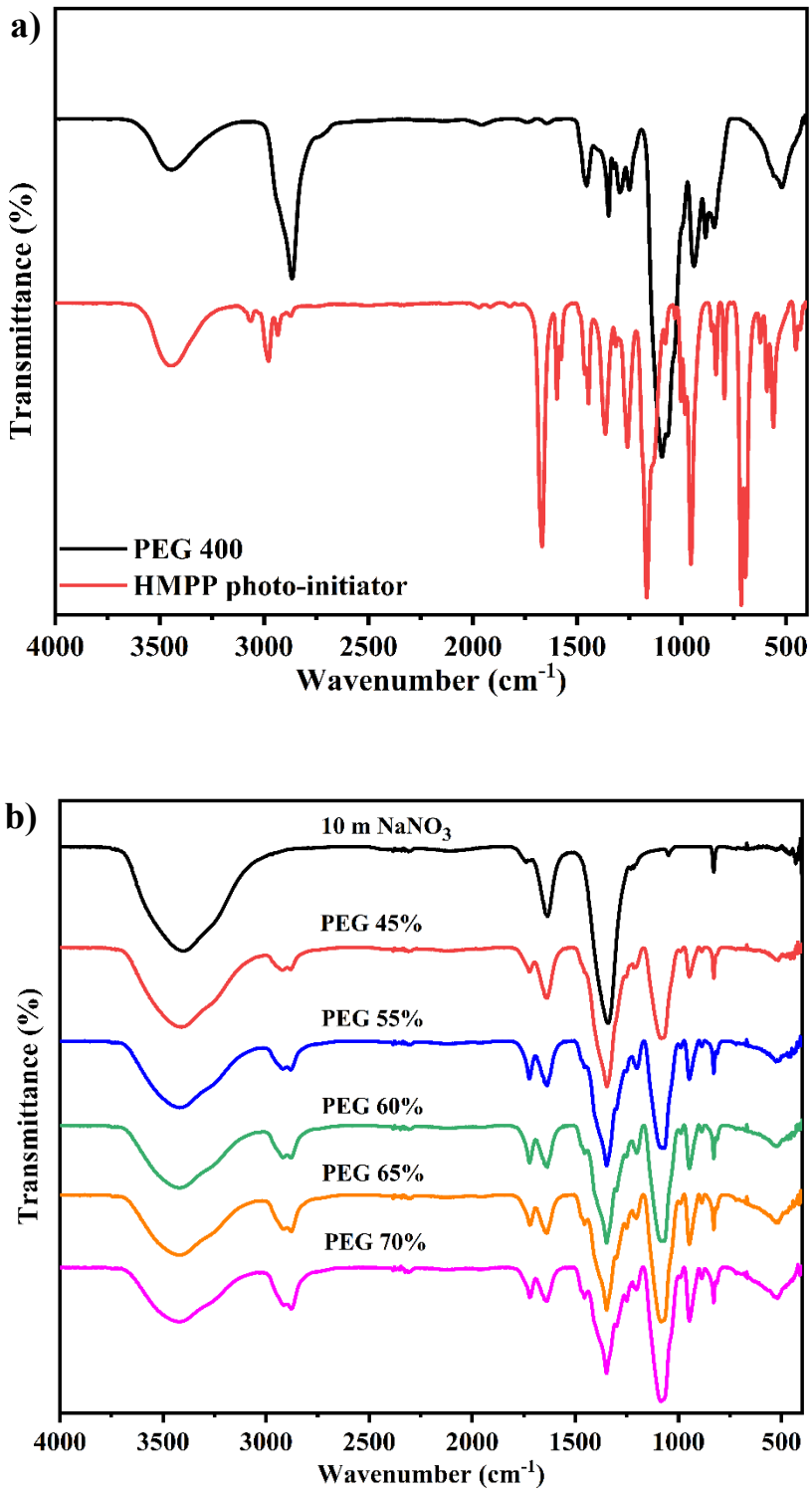

Figure S4. FTIR spectra of a) PEG 400 and HMPP photo-initiator and b) 10 m $NaNO_3$ and precursor solutions.

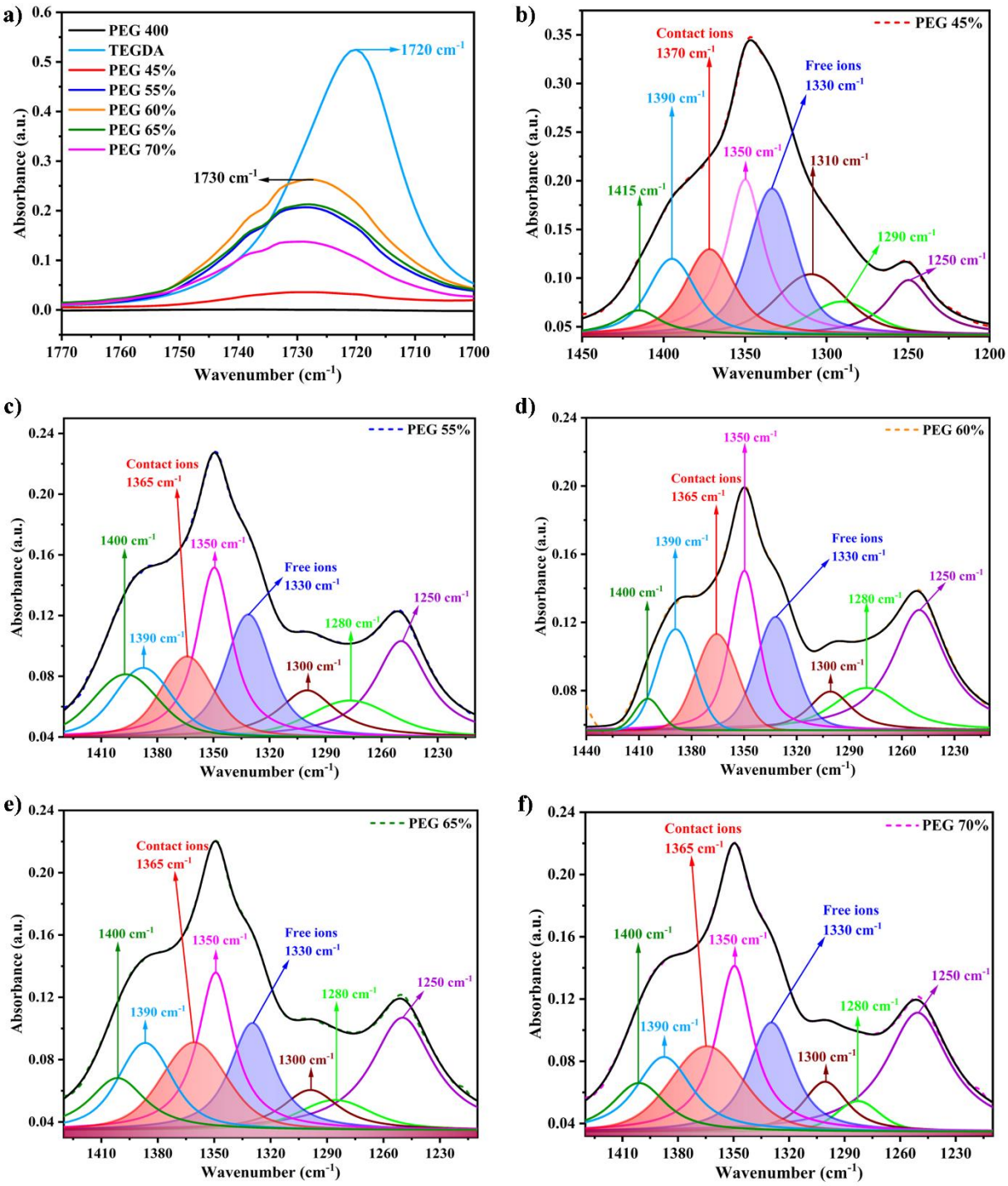

Figure S5. a) FTIR spectrum between 1,770 to 1,700 cm^{-1} for PEG 400, TEGDA, and QSEs with different PEG contents. Deconvolution of FTIR spectra in the wavenumber region of 1,450 to 1,200 cm^{-1} for QSEs with each PEG content of: b) PEG 45 wt%, c) PEG 55 wt%, d) PEG 60 wt%, e) PEG 65 wt%, and f) PEG 70 wt%.

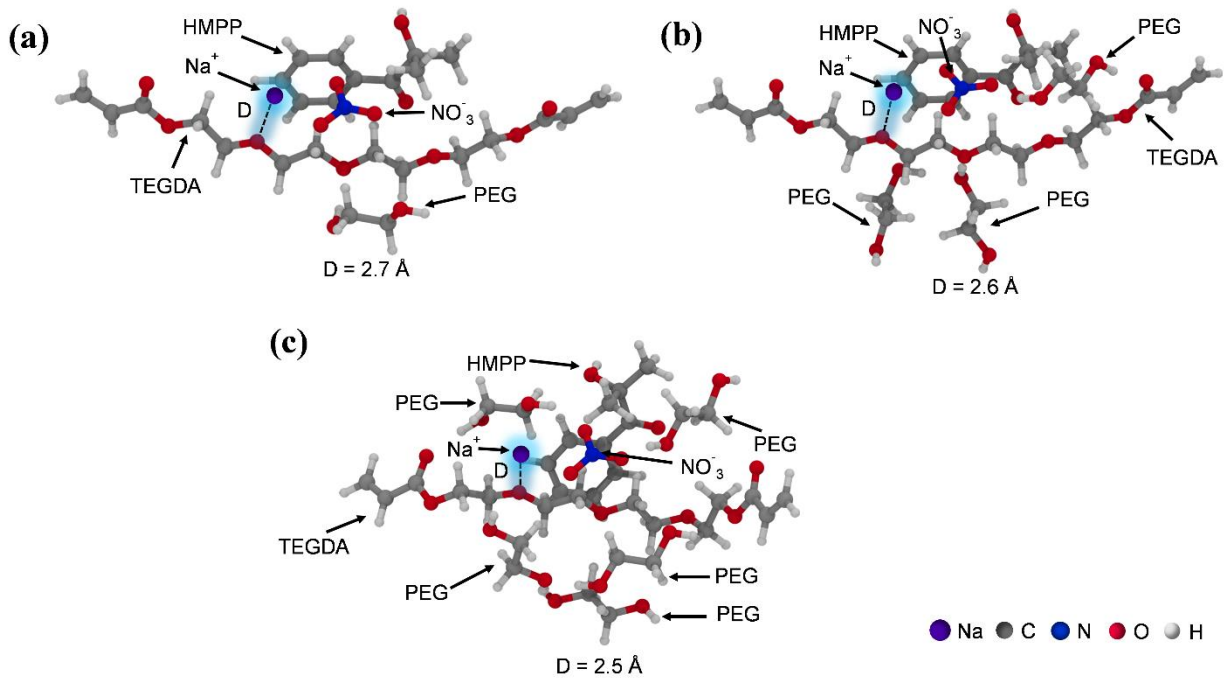

Figure S6. The optimised geometries of TEGDA–PEG–HMPP–$NaNO_3$ complexes with different Na^+–O distances (D), illustrating the effect of increasing PEG content: (a) one PEG molecule, (b) three PEG molecules, and (c) five PEG molecules. The purple, silver, blue, red, and white spheres represent sodium, carbon, nitrogen, oxygen, and hydrogen atoms, respectively.

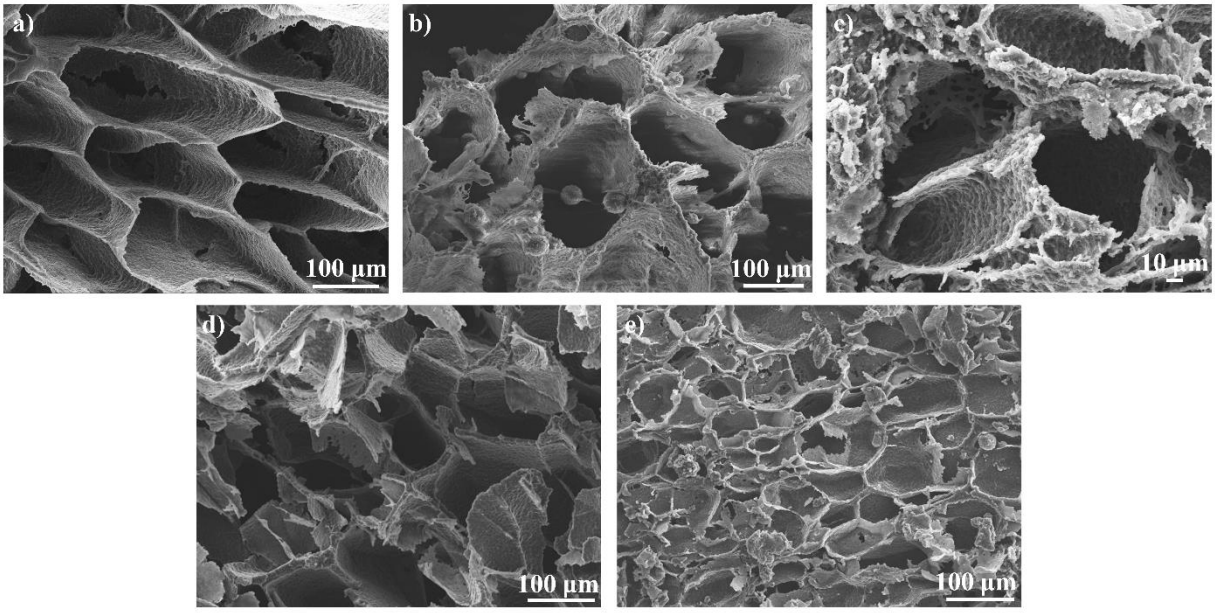

Figure S7. FESEM images of each QSE with different PEG contents of a) PEG 45 wt%, b) PEG 55 wt%, c) PEG 60 wt%, d) PEG 65 wt%, and e) PEG 70 wt%.

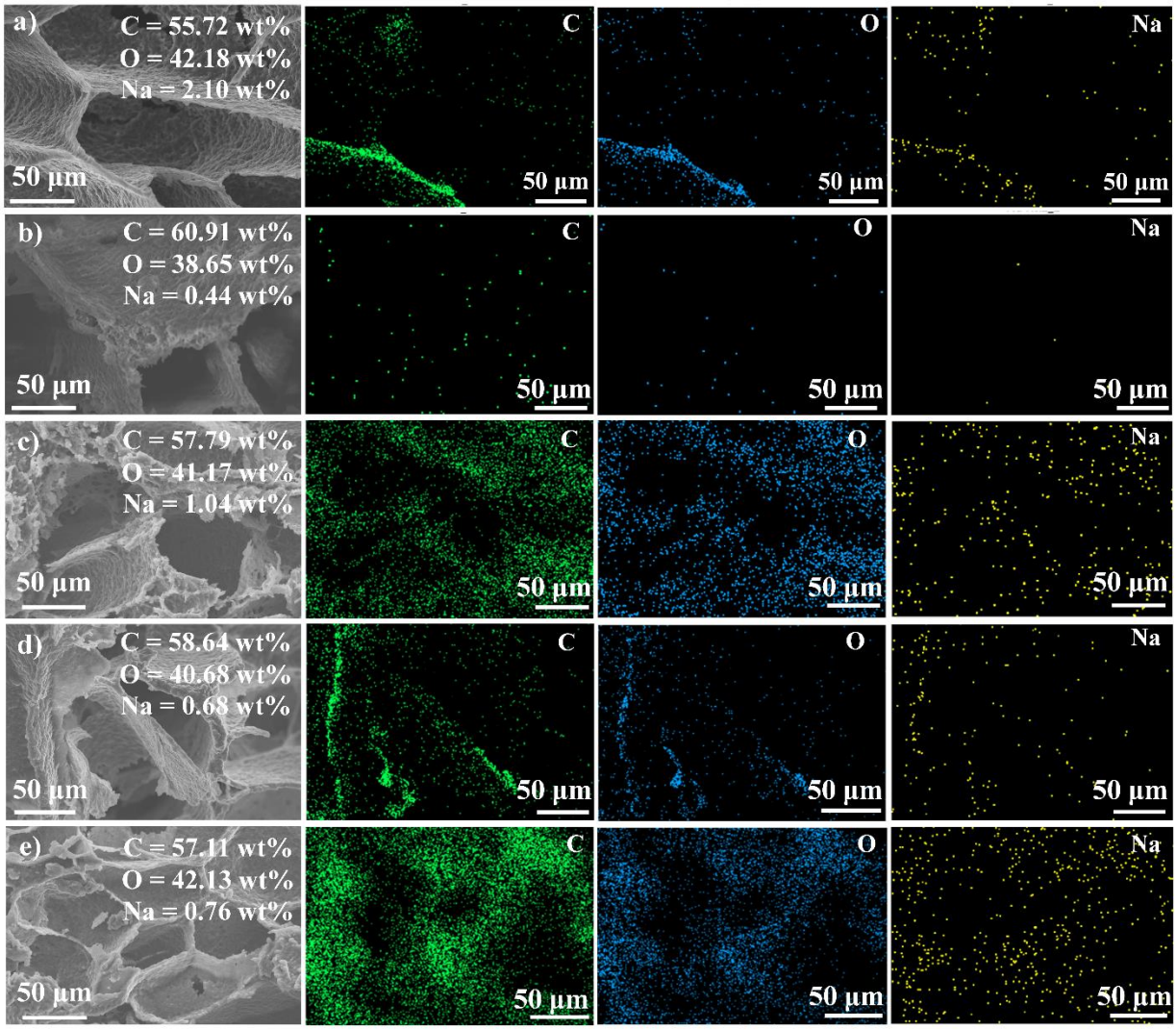

Figure S8. EDS mapping images of each QSE with different PEG contents of a) PEG 45 wt%, b) PEG 55 wt%, c) PEG 60 wt%, d) PEG 65 wt%, and e) PEG 70 wt%.

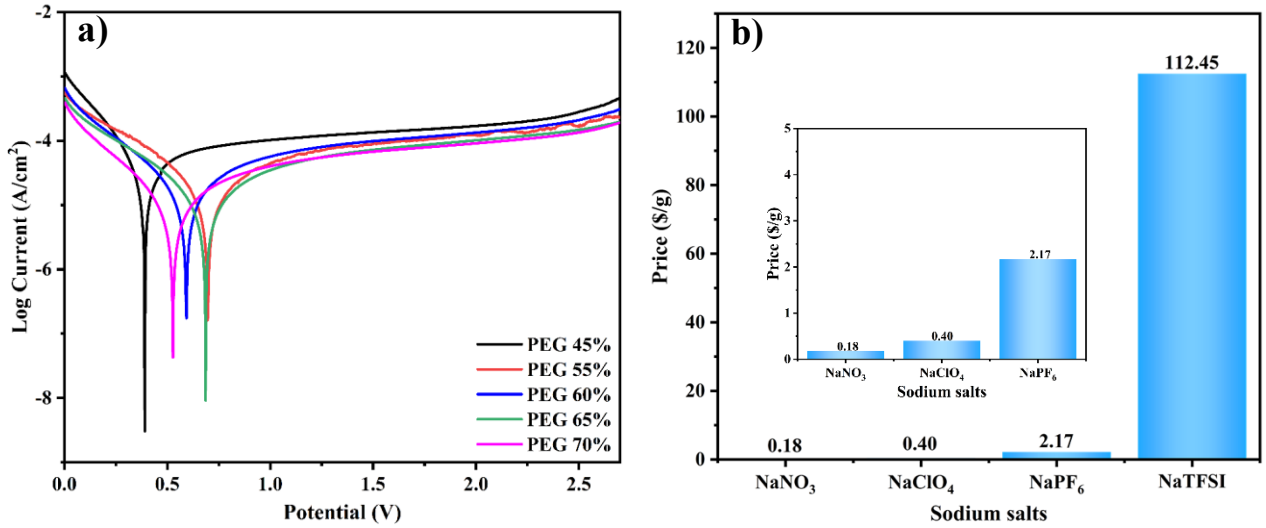

Figure S9. a) Tafel curves of graphite paper in QSEs at various PEG contents and b) Comparison of different sodium salts price from Sigma Aldrich.

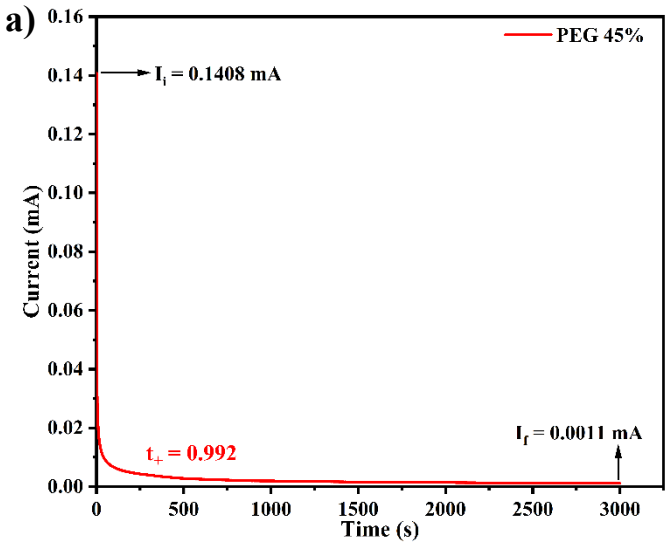
a)
PEG 45%
I_i = 0.1408 mA
I_f = 0.0011 mA
t_+ = 0.992
Current (mA)
Time (s)
0.00
0.02
0.04
0.06
0.08
0.10
0.12
0.14
0.16
0
500
1000
1500
2000
2500
3000

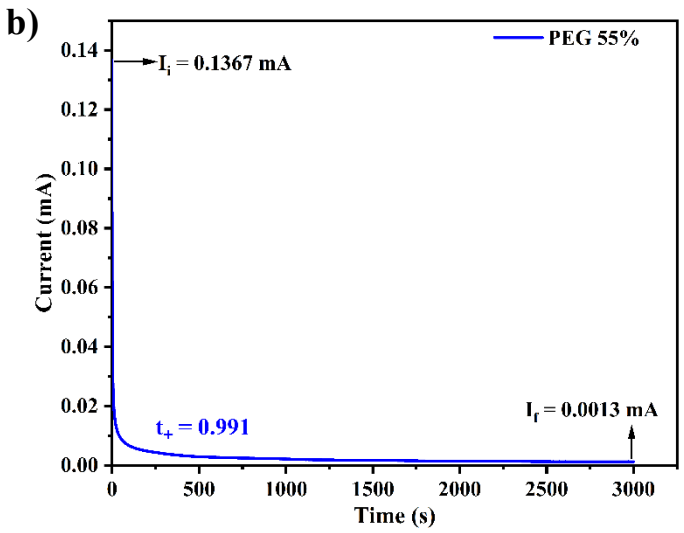
b)
PEG 55%
I_i = 0.1367 mA
I_f = 0.0013 mA
t_+ = 0.991
Current (mA)
Time (s)
0.00
0.02
0.04
0.06
0.08
0.10
0.12
0.14
0
500
1000
1500
2000
2500
3000

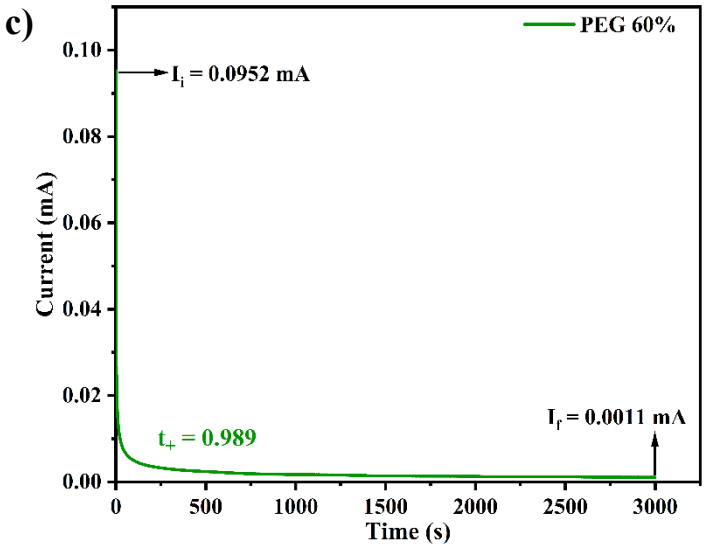
c)
PEG 60%
I_i = 0.0952 mA
I_f = 0.0011 mA
t_+ = 0.989
Current (mA)
Time (s)
0.00
0.02
0.04
0.06
0.08
0.10
0
500
1000
1500
2000
2500
3000

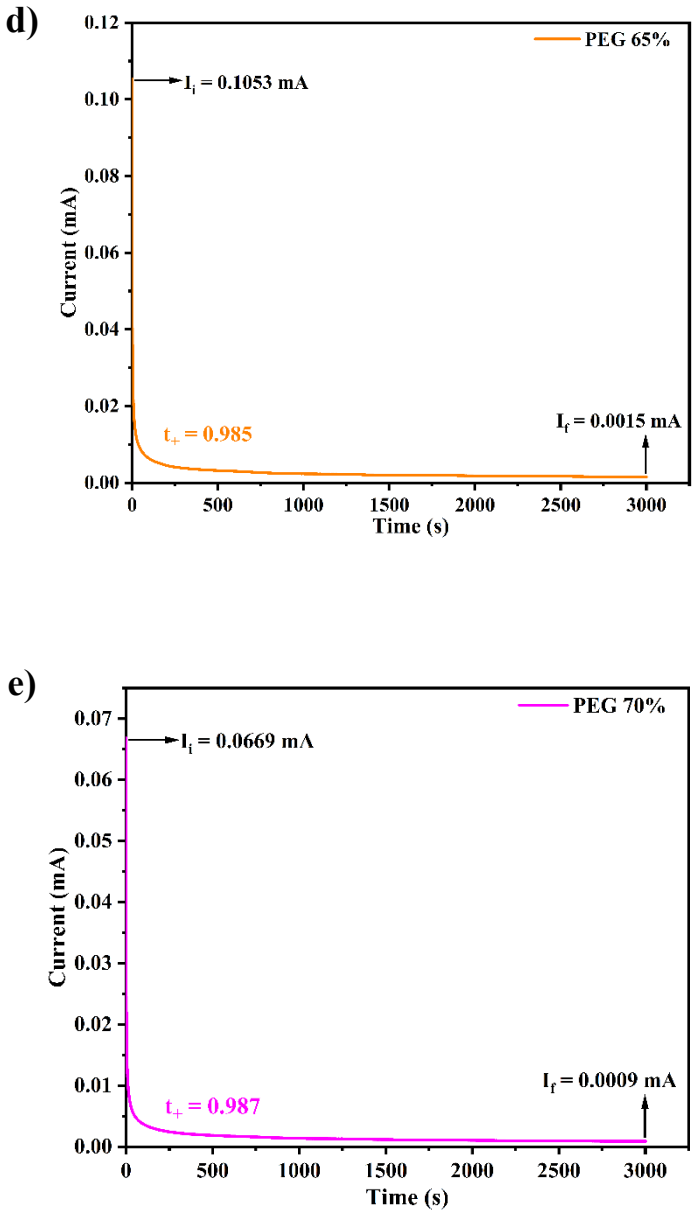

Figure S10. Transference number profiles under 1 V polarization for each QSE with various PEG contents: a) PEG 45 wt%, b) PEG 55 wt%, c) PEG 60 wt%, d) PEG 65 wt%, and e) PEG 70 wt%.

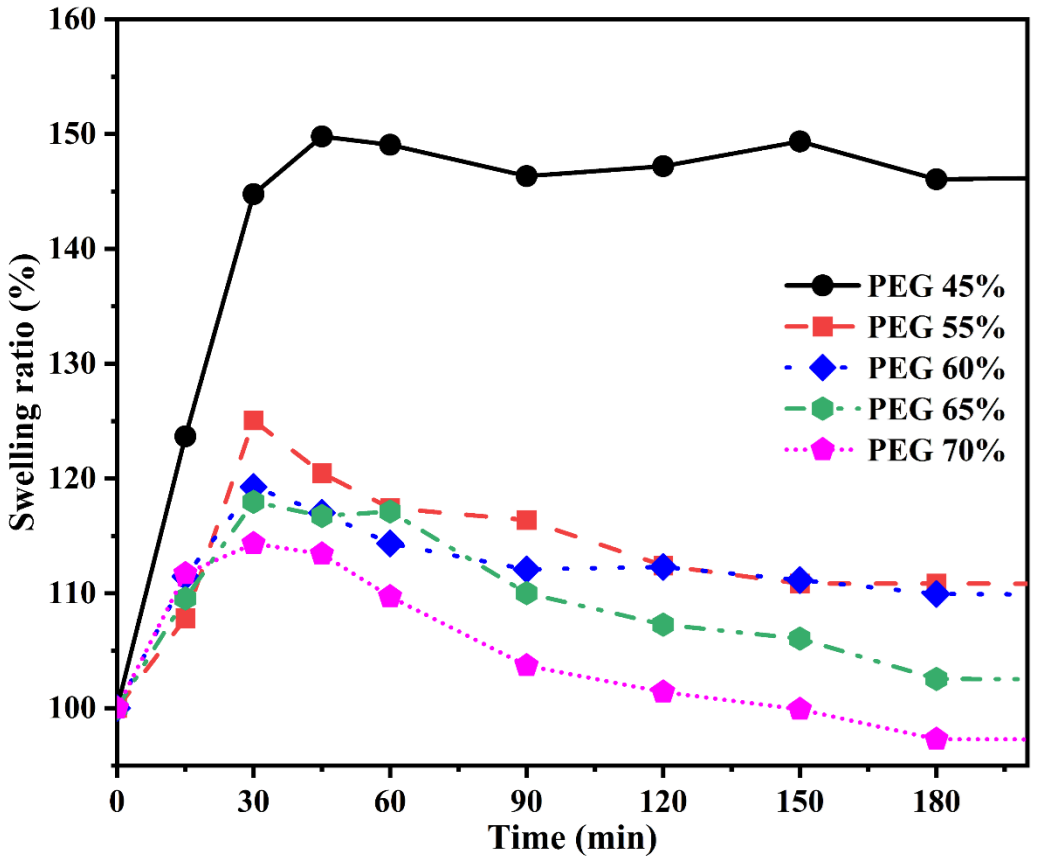

Figure S11. Swelling ratio of the as-prepared QSEs with various PEG contents immersed in DI water at room temperature.

Table S1. The determined transport parameters, including Free ions, contact ions, number density (η), ionic mobility (μ) and diffusion coefficient (D) of QSEs with different PEG contents obtained by means of FTIR deconvolution technique.

PEG contents (wt%)	*Free ions* (%)	*Contact ions* (%)	$\eta \times 10^{22}$ (cm^{-3})	$\mu \times 10^{-7}$ ($cm^2/v{\cdot}s$)	$D \times 10^{-8}$ (cm^2/s)
45	60.871	39.129	1.840	31.187	7.899
55	59.027	40.973	1.513	18.716	4.726
60	56.063	43.937	1.169	21.139	5.355
65	50.122	49.878	1.393	10.908	2.763
70	48.634	51.366	1.341	7.239	1.834

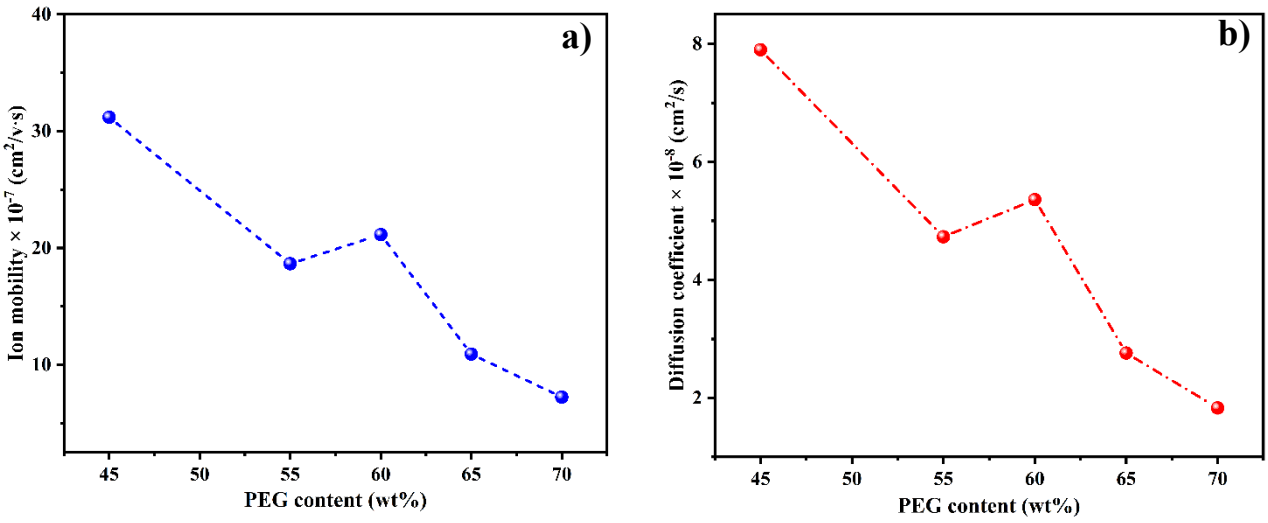

Figure S12. a) Ion mobility and b) Diffusion coefficient at various PEG contents.

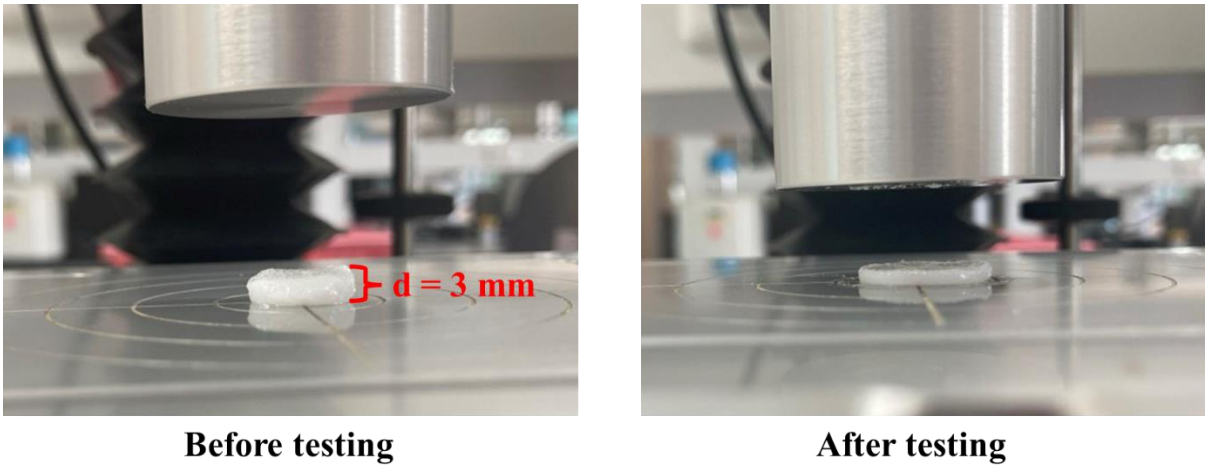

Figure S13. Texture analyzer measurements procedure.

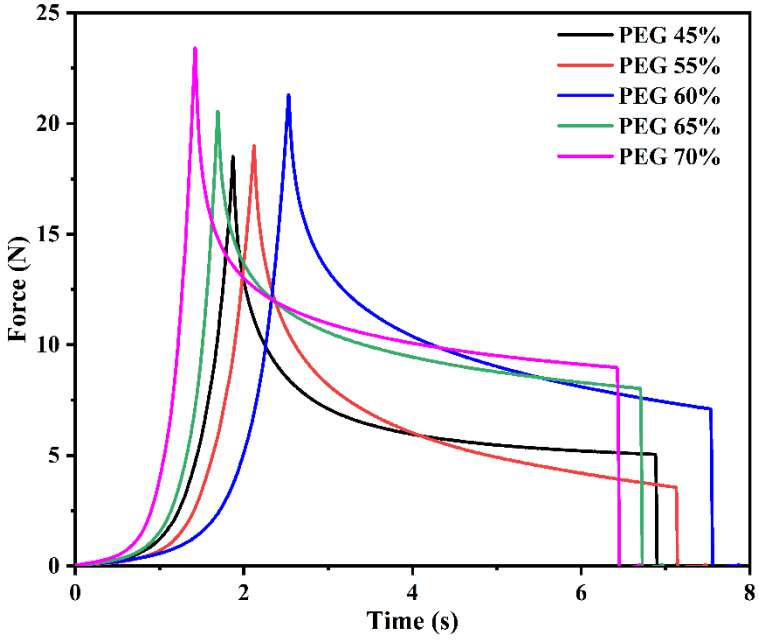

Figure S14. Texture analyser profiles of each QSE.

Table S2. Average Hardness (*H*) and Young's modulus of QSEs at various PEG contents of 45, 55, 60, 65, and 70 wt%.

Sample	*H* (MPa)	Young's modulus (MPa)
PEG 45%	0.136 ± 0.019	2.307 ± 0.250
PEG 55%	0.140 ± 0.005	2.254 ± 0.366
PEG 60%	0.163 ± 0.006	2.960 ± 0.346
PEG 65%	0.155 ± 0.001	2.938 ± 0.139
PEG 70%	0.172 ± 0.006	2.834 ± 0.481

Figure S15. Photograph of the prepared pouch cell assembled between AC electrodes (square shapes of 1×1 cm^2) with an active mass material of approximately 2 mg/cm^2 and the QSEs (thickness of 1 mm).

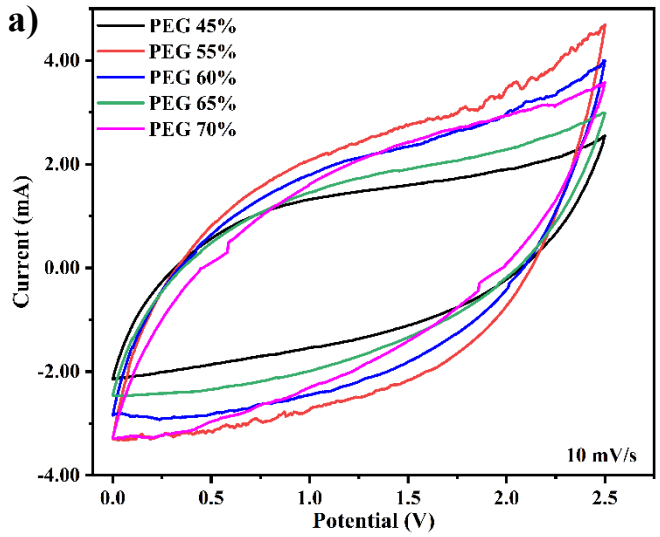
a)
PEG 45%
PEG 55%
PEG 60%
PEG 65%
PEG 70%
Current (mA)
Potential (V)
10 mV/s

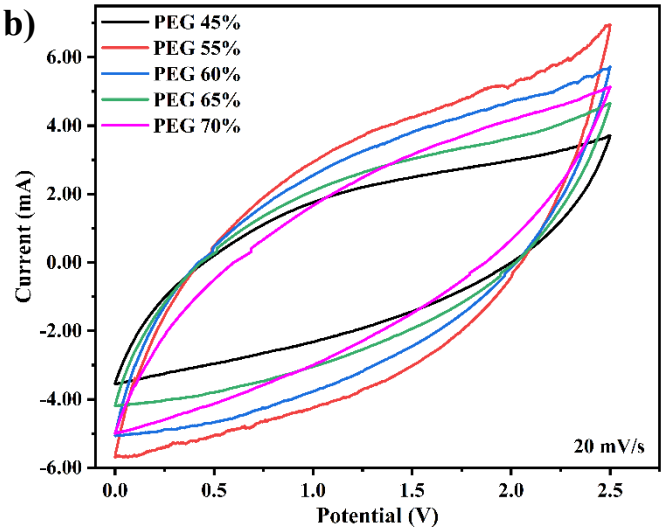
b)
PEG 45%
PEG 55%
PEG 60%
PEG 65%
PEG 70%
Current (mA)
Potential (V)
20 mV/s

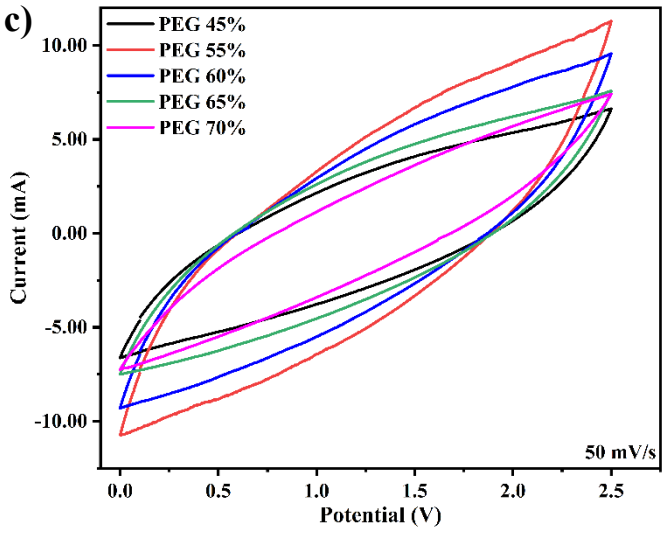
c)
PEG 45%
PEG 55%
PEG 60%
PEG 65%
PEG 70%
Current (mA)
Potential (V)
50 mV/s

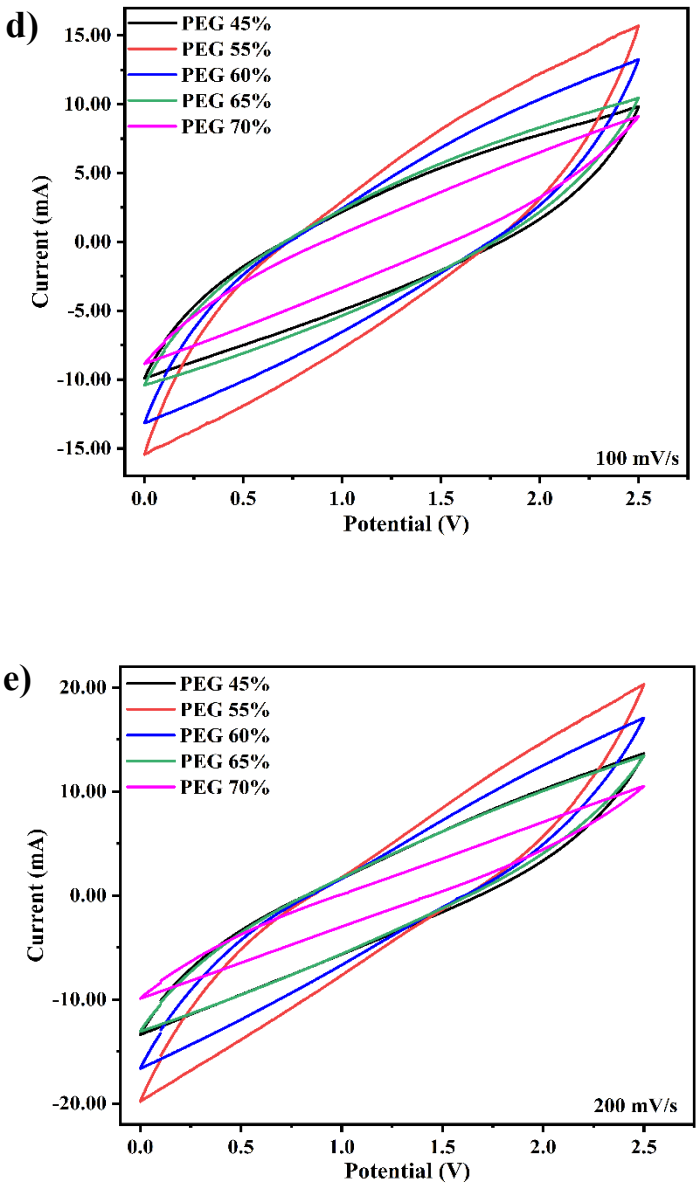

Figure S16. Comparison of CV curves of QSEs sandwiched between AC electrodes at different scan rates: a) 10 mV/s, b) 20 mV/s, c) 50 mV/s, d) 100 mV/s, and e) 200 mV/s.

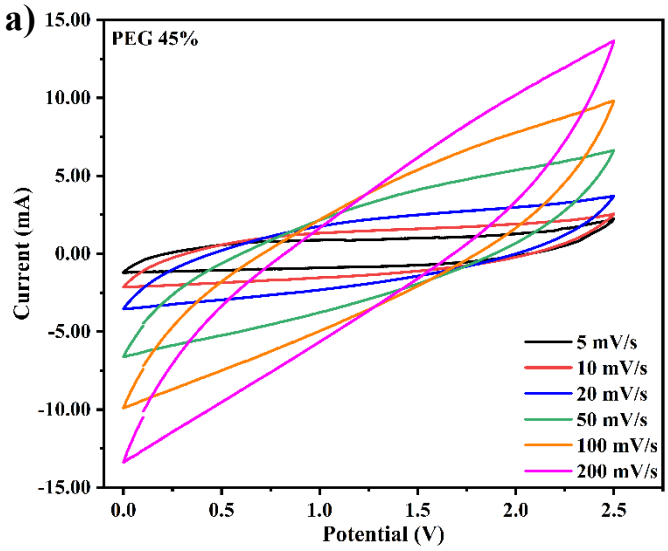
a)
PEG 45%
Current (mA)
Potential (V)
5 mV/s
10 mV/s
20 mV/s
50 mV/s
100 mV/s
200 mV/s

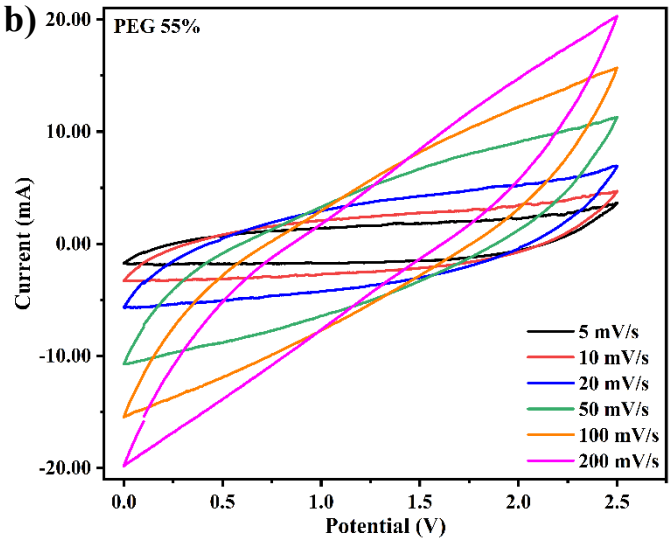
b)
PEG 55%
Current (mA)
Potential (V)
5 mV/s
10 mV/s
20 mV/s
50 mV/s
100 mV/s
200 mV/s

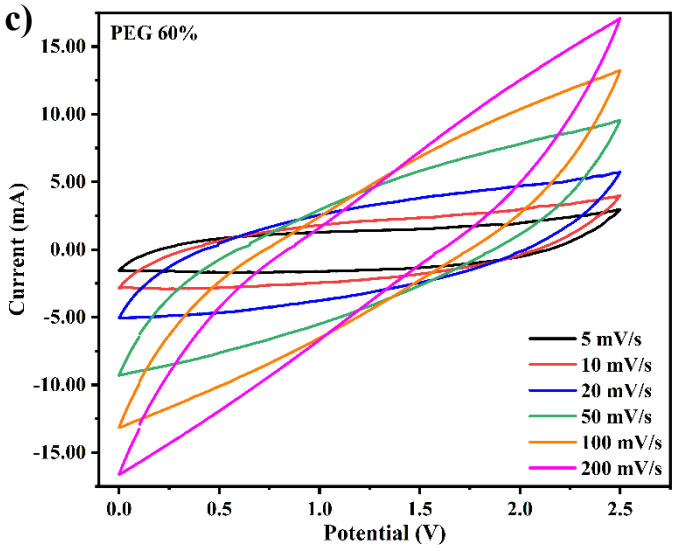
c)
PEG 60%
Current (mA)
Potential (V)
5 mV/s
10 mV/s
20 mV/s
50 mV/s
100 mV/s
200 mV/s

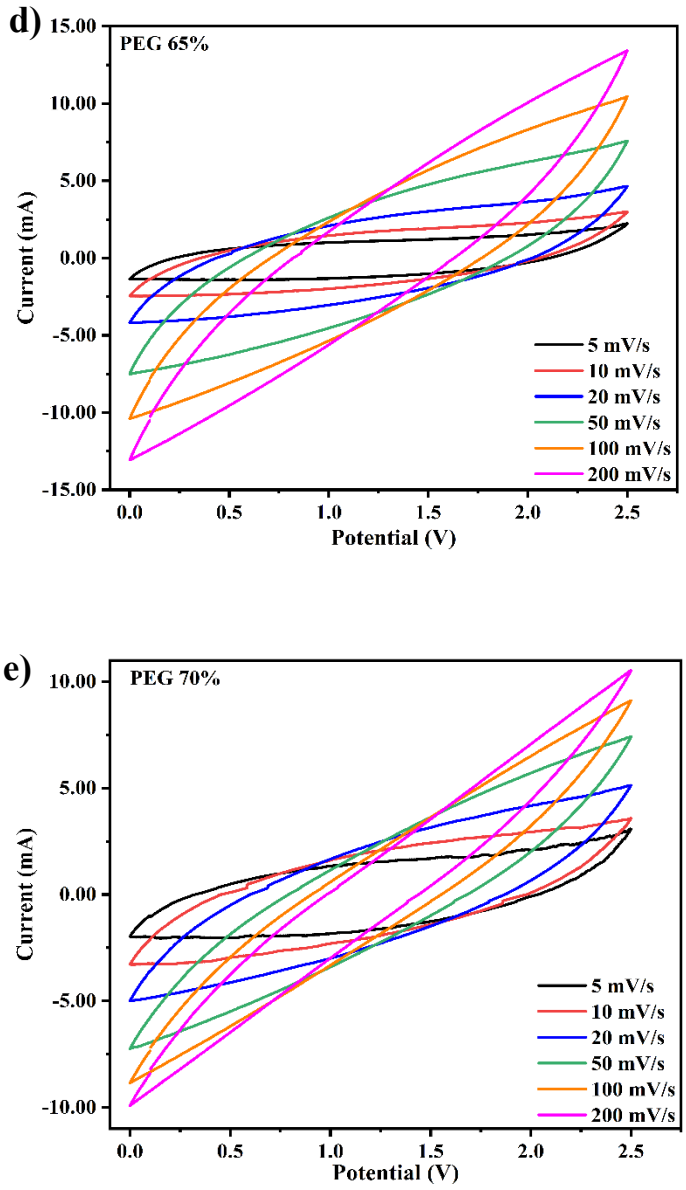

Figure S17. Comparison of CV curves of QSEs with different PEG contents at various scan rates: a) PEG 45 wt%, b) PEG 55 wt%, c) PEG 60 wt%, d) PEG 65 wt%, and e) PEG 70 wt%.

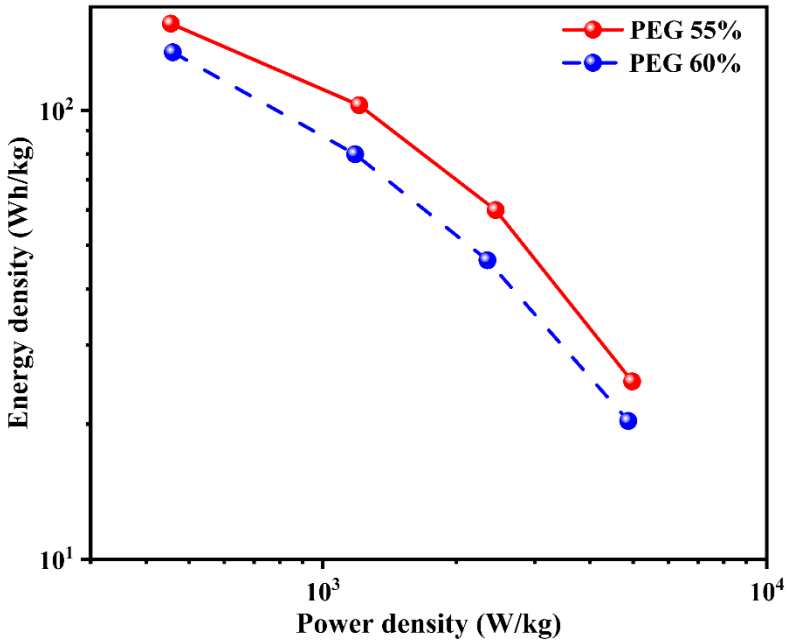

Figure S18. Ragone plot of the symmetric cells assembled with QSEs containing PEG content of 55 and 60 wt% at current densities of 0.2, 0.5,1, and 2 A/g.

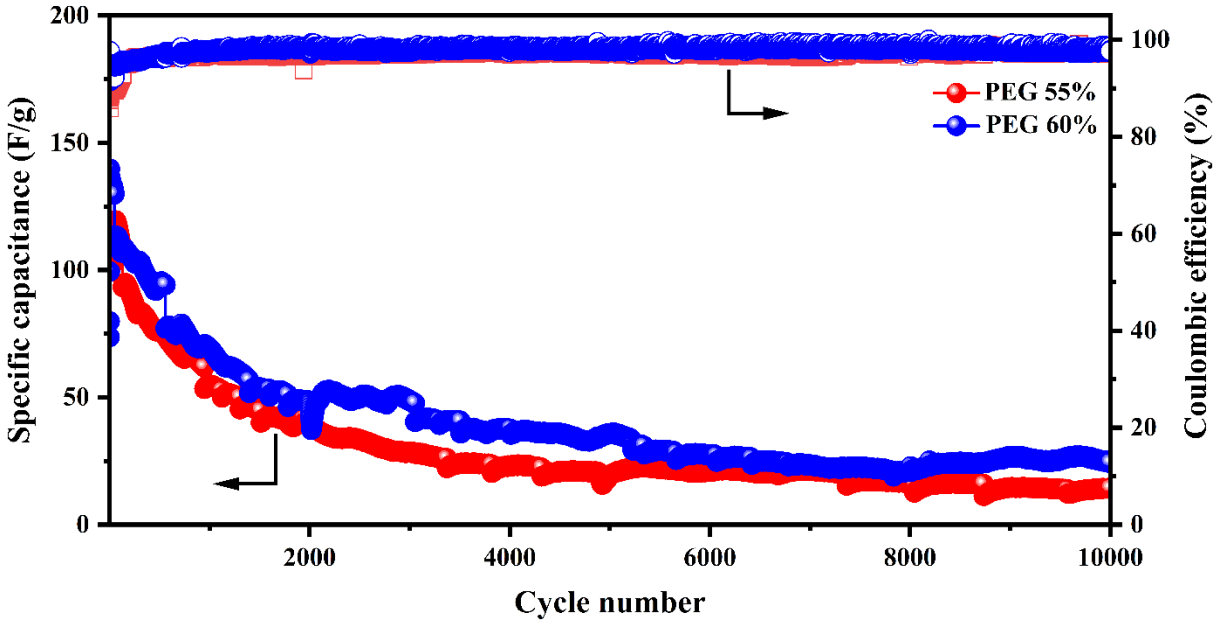

Figure S19. Cycling performance of symmetric cells assembled with QSEs containing 55 and 60 wt% PEG at a current density of 0.5 A/g.

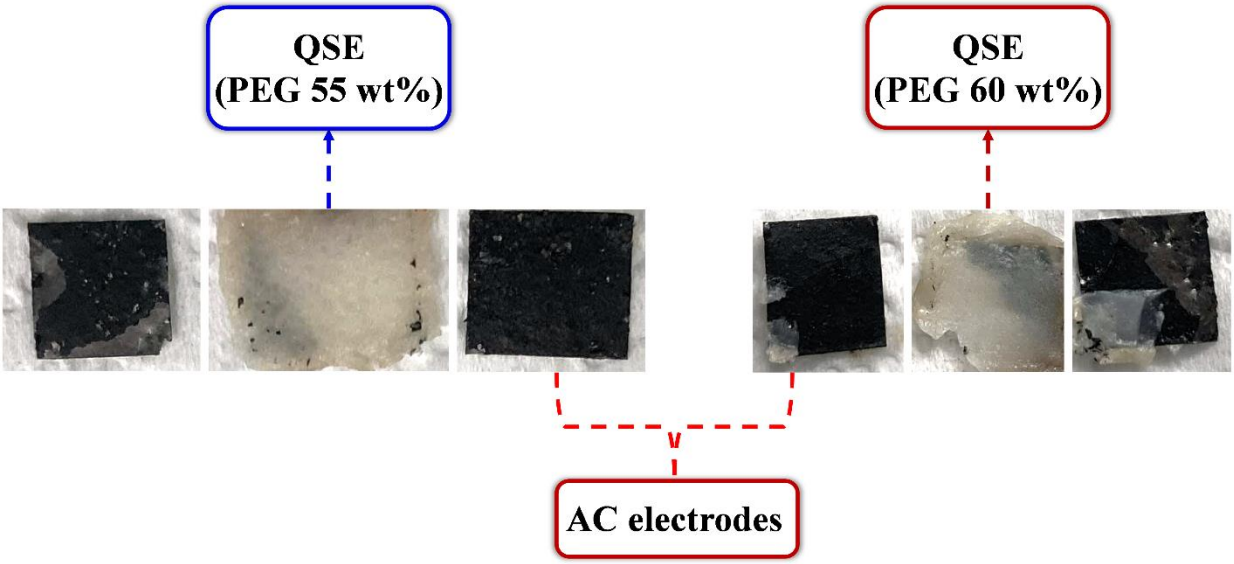

Figure S20. The photograph of opened symmetric cells assembled with QSEs containing 55 and 60 wt% PEG after cycling at a current density of 0.5 A/g.

References

1. R. He and T. Kyu, *Macromolecules*, 2016, **49**, 5637-5648.

2. M. N. Hafiza and M. I. N. Isa, *J. Membr. Sci.*, 2020, **597**, 117176.

3. P. S. Anantha and K. Hariharan, *Solid State Ionics*, 2005, **176**, 155-162.

4. A. K. Arof, S. Amirudin, S. Z. Yusof and I. M. Noor, *Phys. Chem. Chem. Phys.*, 2014, **16**, 1856-1867.